Table IX. Molecular Constants of 2-Azabutadiene[a] (in MHz, u·Å², and D)

	obs	calc	ρ^b
A	47186.010 (23)	49086	1.040
B	4886.5325 (27)	4926	1.008
C	4430.0673 (23)	4477	1.011
Δ	-0.053877 (82)	0.00	
Δ_J	0.000995 (11)		
Δ_{JK}	-0.00801 (29)		
Δ_K	0.3406 (32)		
δ_J	0.00011743 (46)		
δ_K	0.005158 (51)		
μ_a	0.443 (33)	0.42	0.95
μ_b	1.896 (74)	1.64	0.86
μ_c		0.0	
χ_{aa}	0.5 (10)	0.92	1.84
χ_{bb}	-4.4 (11)	-5.14	1.17
χ_{cc}	3.9 (5)	4.22	1.08

[a] Numbers in parentheses represent 3 times the standard deviation attached to the last digits. [b] ρ = calc/obs.

becomes weaker, owing to the existence of hyperfine components. However, hyperfine splitting is useful for spectral assignment if the frequency shifts of the hyperfine components can be estimated with sufficient reliability. In case of a chlorine atom, the quadrupole coupling constants have been estimated empirically, since a cylindrical electron distribution around the bond that connects the chlorine with other atoms may be a good approximation. On the other hand, it is difficult to predict the quadrupole coupling constants of such atoms as nitrogen and boron. Recently, ab initio MO calculations have been able to give reliable molecular constants such as geometry, dipole moments, force field, electronic energy, and so on. Yamanouchi et al.[8] extended the program HONDOG so that it may give quadrupole coupling constants by the use of calculated field gradients. The calculated quadrupole coupling constants have been found to be in good agreement with experimental values.[8,12] The quadrupole coupling constants estimated by ab initio calculation are reliable enough to help the identification of transitions as described in the preceding section.

The ab initio MO calculation based on 4-31G(N*) or larger basis set gives sufficiently reliable geometrical parameters of midsized molecules, although it gives slightly shorter bond lengths since the SCF calculation neglects the effects of electron correlation.[13] The discrepancy comes partly from the experimental limitations. For most of molecules the r_0 or r_s structures are determined experimentally since it is impossible or extremely laborious to determine the equilibrium structures. In fact, the ab initio calculation gives rotational constants slightly larger than the experimental constants. Since the discrepancy lies between 1 and 4% in most cases, the discrepancy between calculated and experimental bond length is estimated to be less than 2%. The present study revealed that not only molecular geometry and electronic energy but also such molecular constants as dipole moments and hyperfine coupling constants can be calculated reliably by ab initio MO methods.

Acknowledgment. We are grateful to Dr. Peter A. Hackett for critical reading of the manuscript.

Registry No. 9, 32115-53-0; **10**, 32360-82-0; **11**, 6788-85-8; **12**, 382369-27-9; $CH_2N^{37}Cl$, 118017-56-4.

(12) Sugie, M.; Takeo, H.; Matsumura, C. *J. Mol. Spectrosc.* **1985**, *111*, 83-92.
(13) Pople, J. A. *Applications of Electronic Structure Theory*; Schaefer, H. F., III, Ed., Plenum: New York, 1977; Chapter 1.

Orientation of NH_3D^+ in Tutton Salt: Equilibrium Orientation and Tunneling Kinetics

Andrew P. Trapani[†] and Herbert L. Strauss*

Contribution from the Department of Chemistry, University of California, Berkeley, California 94720. *Received July 5, 1988*

Abstract: The equilibrium orientation and the kinetics of reequilibration of NH_3D^+ dilute in ammonium cobalt sulfate have been studied as a function of temperature. The equilibrium distribution has been examined by a Monte Carlo simulation and seems to correspond to a partially ordered orientational glass at temperatures below 20 K. To study the kinetics, the orientation distribution is perturbed either by T-jump or by laser spectral hole-burning in the infrared. The kinetics of the reequilibration of the various perturbed distributions are analyzed to find the rate constants for the different elementary reorientation processes of the NH_3D^+ ions. These rate constants show the temperature dependences characteristic of tunneling reactions. These include the range of possibilities from temperature independence to high-power-of-temperature dependence.

I. Introduction

Tunneling is a fundamental part of many chemical rate processes.[1,2] A number of different types of tunneling play a role in chemistry—particularly electron tunneling and nuclear or molecular tunneling. We consider only molecular tunneling in which a group of atoms penetrates through a barrier. Such tunneling has two well-known signatures: the presence of a large kinetic isotope effect and a characteristic temperature dependence. The temperature dependence shows a decreasing activation energy as the temperature is lowered and finally becomes nonexponential or even independent of temperature. It is the low-temperature dependence we have been able to demonstrate for a number of different reactions involving the NH_3D^+ ion dilute in the Tutton salt ammonium cobalt sulfate $[(NH_4)_2Co(H_2O)_6(SO_4)_2$, ACS]. A NH_3D^+ ion can exist in four crystallographically well-defined orientations (i.e., the N–D in one of the four approximately tetrahedrally placed directions) in the ACS crystal. The equilibrium distribution of the NH_3D^+ in these ions in the crystal changes with temperature,[3,4] and we can change the orientation

[†] Current address: Rohm & Haas Co. Research Laboratories, Spring House, PA 19477.

(1) Bell, R. P. *The Tunnel Effect in Chemistry*; Chapman and Hall: London, 1980.
(2) Goldanskii, V. I.; Fleurov, V. N.; Trakhtenberg, L. I. *Sov. Sci. Rev., Sect. B* **1987**, *9*, 59-124.
(3) Trapani, A. P.; Strauss, H. L. *J. Chem. Phys.* **1986**, *84*, 3577-3579.

0002-7863/89/1511-0910$01.50/0

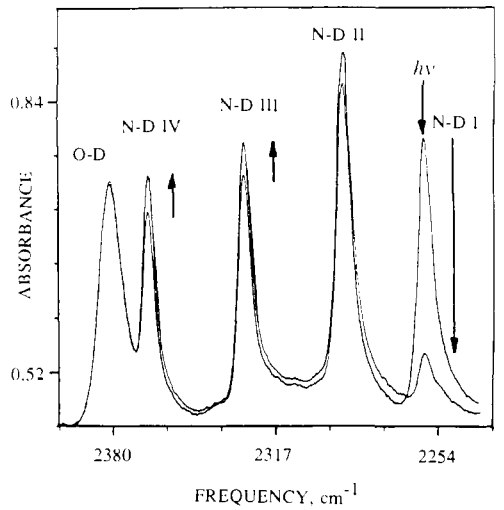

Figure 1. IR spectrum of the N–D stretching region of the NH_3D^+ ion in 4% D ACS at 4 K. Two spectra are superimposed. There are four bands arising from the four different orientations that the NH_3D^+ ions may assume in the crystal. These are numbered from I to IV as shown. The remaining band shown in the figure arises from the O–D stretch of the inevitably present HDO. One spectrum shown was taken before diode laser irradiation of N–D I and the other immediately after 60 min of irradiating the sample with a diode laser tuned to the N–D I frequency. Arrows indicate the direction of the changes in intensity of the IR spectrum. The change in N–D II is due to thermal equilibration during the course of the irradiation and is not caused by the laser-induced process. The laser causes the ions in the orientation corresponding to N–D I to rotate out of that orientation and assume one of the orientations corresponding to N–D III or N–D IV. Note that the O–D band does not change, as it should not, if the assignment of the spectrum is correct.

of the ions either by changing the temperature (T-jump)[4] or by laser irradiation of one of the N–D stretching bands (structural hole-burning).[5,6] We can then follow the reequilibration of the ammonium ions to their equilibrium distribution. At low temperatures, this reequilibration takes place by tunneling.

The population of each site can change by moving to one of the other three sites. We analyze our kinetic data to approximately determine the individual rate constants involved. We emphasize that our measurements are for rates among sites that are crystallographically well characterized.

Before attempting to understand the kinetics, it is necessary to consider the equilibrium orientation of the NH_3D^+ ions. The NH_3D^+ ions sit in crystal sites with the hydrogen atoms hydrogen bonded to the oxygens of the surrounding sulfate ions. As the temperature is lowered toward 30 K, the NH_3D^+ ions progressively order. That is, more of the N–D bonds populate one specific orientation. Below this temperature, the extent of ordering remains fixed. A model of independent ammonium ions rotating among sites of slightly different energy will lead to an extent of ordering that continually increases with decreasing temperature, and so in our previous work,[3,4] we have modeled this ordering as due to interactions among the dipole moments of the NH_3D^+. This provided a rationale for the observed behavior, albeit a very approximate one. In this paper, we improve our model by making the dipole moment orientation dependent. The calculations with this model provide some insight into the possible structure of the low-temperature ordered NH_3D^+ network.

The experimental analysis of the NH_3D^+ orientations uses the N–D stretching region of the infrared spectrum (Figure 1). As shown in the figure, there are four N–D stretches corresponding to the D in one of the four possible inequivalent sites. We number the infrared bands from I to IV. The D sites are numbered similarly. We know the correspondence between the spectral bands and the crystallographic positions, because there are empirical correlations between the N–D–O distances and infrared frequencies.[4] (The O atom is from the SO_4 groups to which the ammonium ions hydrogen bond.) Irradiating one of the stretch bands with a lead-salt diode laser allows us to "hole-burn", changing the orientation distribution of NH_3D^+ ions (Figure 1 and ref 5 and 6). In principle, we can burn each of the N–D bands in turn to obtain different nonequilibrium distributions and different rate constants. It is the reequilibration process and its temperature dependence that we report on in the second half of this paper.

The observed reequilibration of the spectral bands is analyzed to give the rates of reaction between individual sites. The barrier to reorientation is ~4 kcal/mol and the temperatures we consider are lower than 30 K. The Arrhenius factor $\exp(-\Delta E^{\ddagger}/kT)$ is then 10^{-29} or less, and thus, the reequilibration we observe must be due to tunneling. The temperature dependence of the rates arises from interaction of the orientational degrees of freedom with phonons, that is the vibrations of the surroundings of the ammonium ion. Our analysis yields an approximate picture of these interactions.

II. Experimental Section

The kinetics experiments were performed on ACS containing 4% deuterium. The deuterium-doped ACS was synthesized in the manner described in ref 4. The ACS was prepared for infrared studies by mulling it with Fluorolube (a fluorochlorocarbon grease) and then sandwiching the mull between two calcium fluoride plates. The FTIR spectrometer used in these experiments was a Nicolet HV8000 modified to allow us to carry out laser irradiation of the sample.[6]

Previously, we measured the time response of the NH_3D^+ orientation distribution to a temperature jump through the order–disorder transition. These experiments were carried out in a Janis Supervaritemp liquid helium Dewar. The Janis Dewar is capable of making rapid temperature changes (on the order of minutes), but is not convenient or economical for maintaining a sample at cryogenic temperatures for longer than 12 h. At 4.2 K, the NH_3D^+ orientation distribution reequilibration occurs with a time constant on the order of 10 h. Therefore, the resulting reequilibration time constants measured in the temperature-jump experiments are not determined as accurately as they might be. This inaccuracy contributed to our inability to detect a temperature dependence for the time constants measured by these experiments.[4]

Now, we have been able to measure the solid-state NH_3D^+ ion reorientation kinetics over periods of a week by making use of a CTI closed-cycle helium refrigerator, Model SC21, a Lakeshore Cryotronics temperature controller, Model DTC 500-SP, and the ability to selectively reorient the NH_3D^+ ions with an IR laser. We cooled the ACS samples to below 30 K in the CTI refrigerator. The refrigerator was then mounted in the FTIR spectrometer. After the refrigerator had cooled the sample to the desired temperature (a process that may require as long as 2 h), we prepared a nonequilibrium NH_3D^+ orientation distribution by structurally hole-burning the sample in the manner detailed in ref 5 and 6. The structural hole-burning allowed us to selectively rotate NH_3D^+ ions out of one orientation and into one of the three other possible orientations (Figure 1). The nonequilibrium state thus created slowly reequilibrates, a process we followed by periodically measuring the IR spectrum of the sample. Our past experience had shown that the FTIR spectrometer source (a 1400-K globar) could speed up the NH_3D^+ reequilibration by as much as a factor of 2 if allowed to continuously strike the sample. Therefore, the structural hole-burning prepared sample was reequilibrated in the dark; the IR spectrometer source only struck the sample when a spectrum was actively acquired. This required only ~50 s out of every 1 h at the beginning of the experiment and only 50 s out of every 6 h near the end, a negligible exposure. This experimental protocol provides a means for accurately determining the temperature dependence of the NH_3D^+ reorientation kinetics. We have only been able to burn N–D bands I and II because our laser cuts off above 2300 cm^{-1}. The technology of lead-salt diodes is improving rapidly, and we hope to do the kinetics experiments with burning III and IV in the near future.

III. Calculation of the Equilibrium Distribution

The NH_3D^+ ions in an ammonium Tutton salt sit in completely asymmetric crystal sites (C_1 symmetry). This affords the NH_3D^+ ion four distinct orientations, each of which gives rise to a distinct

(4) Trapani, A. P.; Gensler, S. W.; Strauss, H. L. *J. Chem. Phys.* **1987**, *87*, 4456–4464. There is an error in the calculated temperature scale in Table III. The temperatures listed are the temperatures below which the simulation no longer changes. These temperatures should be 5×10^{-6}, 3×10^{-5}, 1.6×10^{-5}, 1.6×10^{-3}, and 1.2×10^{-5} K, respectively. The scale in Figure 9 should be multiplied by a factor of 320. Note that these calculated temperatures are still much too low.

(5) Trapani, A. P.; Strauss, H. L. *J. Chem. Phys.* **1987**, *87*, 1899–1900.

(6) Weier, Jane E.; Trapani, Andrew P.; Strauss, Herbert L. *Spectroscopy* **1988**, *3*, 47–49.

N–D stretching band in the IR spectrum of a deuterium-doped ammonium Tutton salt. In the past we showed that the orientation distribution of the NH_3D^+ ions of the ammonium Tutton salts varies as a smooth function of the temperature between 75 and 30 K; between 30 and 2.8 K the orientation distribution becomes temperature independent.[4] The change in orientation distribution between 75 and 30 K indicates a temperature-induced ordering of the NH_3D^+ population. This ordering is partial; only ~40% of the NH_3D^+ population is in the band II orientation at 30 K. Furthermore, the width of the transition region (75–30 K) is deuterium concentration dependent: a higher deuterium concentration results in a wider transition region.[4] The center of the transition also appears to be deuterium concentration dependent. The barrier to rotation between the orientations of the ammonium ions is high, on the order of 4 kcal/mol. Therefore, the tunneling frequency is small, and for an energy level low in the potential well, the molecules are localized in only one of the orientations.

We studied the NH_3D^+ interactions with a Monte Carlo computer simulation. The simulation is classical, an approximation that should be reasonable, since the tunneling frequency is small and the degree of localization high. The interactions were taken to be dipole–dipole. An NH_3D^+ ion can have a permanent dipole moment since the center of mass of the NH_3D^+ ion (as opposed to the NH_4^+ ion) is not located at the center of charge. On this basis, we estimate the dipole moment of a gas-phase NH_3D^+ ion to be 0.253 D.

A model lattice having the geometry of an ammonium Tutton salt was created, and the NH_3D^+ ions were modeled as dipoles of up to 0.7 D. This range of values was estimated by considering the deuterium concentration dependence of the transition temperature and brackets the estimated value of the dipole moment of the gas-phase NH_3D^+ ion. Because the crystal environment of an NH_3D^+ ion may augment or attenuate the effective dipole moment of the ion, it is difficult to calculate the value of the true solid-state NH_3D^+ dipole moment.

After the model lattice was randomly seeded with N–D dipoles, the dipoles were allowed to interact by use of the Monte Carlo Metropolis algorithm,[7] with the same calculation techniques as in our previous work.[4] The calculation is characterized by only one dimensionless parameter, the ratio of the dipole–dipole energy to the temperature. The dipole–dipole energy is proportional to the product of the dipole moment squared divided by the average of the effective distance between dipoles cubed. The effective distance depends on the geometry of the lattice and the concentration of dipoles.

We showed previously that our simulation of N–D dipoles interacting on a Tutton salt lattice could reproduce the type of orientational order–disorder transition observed with IR spectroscopy. One sees that at high simulation temperature, the orientation distribution is uniform; 25% of the NH_3D^+ population is in each of the four possible orientations. As the temperature is dropped, one orientation is preferentially populated. At the lowest temperature, when the model can no longer change, one sees that the orientation distribution is close to the 4 K–20 K orientation distribution obtained from the IR equilibrium experiments. Regardless of the initial seeding, a population split of about 35:22:22:22 results at the lowest of the reduced temperatures. This result is nearly insensitive to D concentration. The specific orientation populated by 35% of the N–D dipoles is variable, although it was usually orientation II.

The major flaw of this model is that the resulting transition region is too wide. In the real system, the transition region is ~30 K wide, while in the old simulation it is ~4 orders of magnitude wide. The absolute temperature scale of the simulation is also wrong. Thus, it is unlikely that the dipole–dipole forces alone are responsible for the interaction of the ions. It is likely that the interaction between the ions is, at least partly, due to forces of considerably shorter range. We have no explicit form for these forces, as they must involve the sulfate and $Co(H_2O)_6^{2+}$ ions as well. The dipole–dipole model is simple and may well give the correct angular dependence to the interionic forces. As already mentioned, it does reproduce the observed amount of orientation at low temperatures, and so we have refined it to obtain a picture of the partially oriented low-temperature crystal.

Table I. Equilibrium Orientation Distribution

I:II[b]	temp,[c] K	% NH_3D^+ population having orientation[a] I	II	III	IV
0.00	10^{-4}	0	100[d]	0	0
0.50	10^{-1}	13.8	63.5	8.9	13.8
0.75	10^{-3}	22.1	48.4	16.4	3.1
0.88	10^{-3}	21.7	42.5	19.1	16.7
0.94	10^{-3}	16.8	41.3	21.7	20.3
0.97	10^{-3}	18.4	35.0	19.4	27.2
expt[e]	≤20	18.2	40.7	17.6	21.2

[a] Monte Carlo results for ACS crystal structure; 0.75% D (equivalent to 3% ammonium ions with one deuterium). [b] Ratio of the orientation I, III, or IV N–D dipole moment to the orientation II dipole moment. Dipole moment II held constant at 0.7 D. [c] The orientation distribution is calculated to be constant at this and lower temperatures. [d] See Table II for more detail. [e] Experimental population. These numbers differ a bit from those of ref 4 because these include additional data. The numbers do not quite add up to 100%, an indication of the error involved in obtaining the conversion factors between the IR intensities and the populations.

In order to improve the agreement between the computer data and the IR data, we modified the simple N–D dipole simulation described above by making the N–D dipole moment orientation dependent. We used the experimental low-temperature NH_3D^+ orientation distribution and the IR laser-induced NH_3D^+ reorientation as guides in assigning the magnitude of the N–D dipole moment for each of the four possible dipole orientations. The IR spectra show that something is unique about orientation II; below ~30 K, this orientation is the most populated. The remainder of the NH_3D^+ ions populate the other three orientations about equally. The IR laser irradiation experiments reveal the existence of an approximate C_3 symmetry axis about the N–D bond II (see ref 5 and 6). The X-ray crystal structure determination[8] also suggests a unique role for orientation II. The N–H bond lengths given by this study at room temperature are determined by the effect of large-amplitude vibrations and give a different apparent value for N–D II (1.24 Å) than for N–D I, III, and IV (average of 0.60 Å). Thus, we made the moment of an N–D dipole in orientation II larger than that of an N–D dipole in the other orientations and set the moments for N–D dipoles in orientations I, III, or IV equal. The ratio of an orientation II dipole moment to an orientation I, III, or IV dipole moment was taken as an adjustable parameter and used to fit the computer simulation results to the data.

We set the dipole moment for orientation II constant at 0.7 D. We then ran the simulation with varying strengths of the dipole moment for orientations I, III, and IV. We always ran these simulations with a deuterium concentration of 0.75% D (which corresponds to ~120 N–D dipoles for our model size). With a fixed model size, this low concentration allowed for fast computer execution times. The low temperature limiting N–D dipole orientation distribution as a function of the ratio of the orientation II dipole moment to the dipole moment for the remaining orientations is listed in Table I. This table also lists the experimental values. When there is no dipole moment for N–Ds in orientation I, III, or IV, all of the N–D dipoles try to assume orientation II at low temperatures (Tables I and II). Therefore, the dipoles must be forming an energy-lowering network of interactions. If the network could only consist of high-energy interactions, then the N–D dipoles would prefer not to have a dipole moment and would populate orientations I, III, or IV. The ammonium ions in a Tutton salt are related to one another by inversion centers

(7) Metropolis, N.; Rosenbluth, A. W.; Rosenbluth, M. N.; Teller, A. H.; Teller, E. *J. Chem. Phys.* **1953**, *21*, 1087–1092.

(8) Montgomery, H.; Lingafelter, E. C. *Acta Crystallogr.* **1964**, *17*, 1478–1479.

Table II. Calculated Orientation Distribution

% ammonium sites with dipole	temp, K	% NH_3D^+ population having orientation[a]			
		I	II	III	IV
3.0	10^{-4}	0	70–100[b]	0	0
25.0	10^{-1}	5.0	80.0	6.5	8.5
50.0	10^{-2}	10.6	69.2	11.1	9.0
100.0	10^{-1}	13.1	58.3	15.8	12.7

[a] Monte Carlo results for ACS crystal structure. Orientation-dependent dipole moment fixed at N–D II = 0.7 D and N–Ds I, III, and IV = 0.0 D. D concentration dependence of the limiting low-temperature distribution. [b] When the N–D dipole concentration is very low, the amount of population in the favored orientation (II) becomes dependent on the initial seeding of the lattice. The population not in orientation II is evenly distributed among orientation I, III, and IV.

(located on the hydrated metal ions) and translation operations. The translations and inversion centers make it possible for the N–D dipoles to be pointing in spatially opposite or parallel directions while still being in the same crystallographic orientation (such as II, for example).

Depending on the initial seeding of the ammonium sublattice with N–D dipoles, it may or may not be possible for all the dipoles to participate in energy-lowering interactions and be in orientation II. There appears to be some inherent frustration[9] to attaining an all energy-lowering N–D dipole interaction network. We examined this frustration by running a series of simulations where the distribution of dipole moment strengths was constant (N–D II = 0.7 D, N–Ds I, III, IV = 0.0 D), but the percentage of ammonium lattice points occupied by N–D dipoles was varied. The results of these simulations may be found in Table II. Note that 0.75% D listed in Table I is equivalent to 3% of the N–hydrogen lattice sites being occupied by N–D dipoles in Table II. Table II shows that as the N–D dipole concentration goes up, it becomes more difficult to obtain an all energy-lowering dipole network, and thus, it becomes energetically favorable not to have a dipole moment. The 100% N–D dipole simulation on Table II shows that most of the nearest-neighbor dipole interactions can be energy lowering, but the crystal structure does not allow for them all to be so.

In order to further examine the frustration in the dipole–dipole interaction network, we examined all of the N–D II to N–D II dipole interactions within one unit cell from a probe N–D II dipole. This includes dipole separation distances out to ~20.0 Å. Within this chunk of a Tutton salt, 50% of the N–D II to N–D II dipole interactions are energy lowering and 50% are energy raising. The average separation between NH_3D^+ ions in 0.75% D ACS is ~10 Å. There are 24 sites within 10 Å of a central probe N–D II dipole. Of these 24 sites, 16 have N–D II to central probe N–D II interactions that are energy lowering. Within 8.000 Å of a probe N–D II dipole, there are 11 N–D sites; 8 of these yield an energy-lowering interaction to the central site. This shows that the crystal structure appears to favor the formation of small domains consisting of mainly orientation II dipoles. At high N–D dipole concentrations, examination of the model lattice shows that there are indeed domains of II dipoles that are spaced out by areas where the dipoles take a zero dipole moment by assuming orientation I, III, or IV. In this series of simulations (Table II), as the N–D dipole concentration is lowered, the low-temperature occupancy of orientation II increases. Thus, at low dipole concentrations free space can be used to form the buffer zones between N–D II dipole domains and fewer dipoles need assume a 0.0 D orientation.

As the common dipole moment for orientations I, III, and IV is slowly turned on (Table I), it is sometimes favorable for dipoles to assume one of these three orientations so that 100% of the N–D dipoles are no longer in orientation II (Table I). Again, as in the case of zero type I, III, and IV dipoles, the placement of the N–D dipoles does not always allow for an energy-lowering alignment of the strongest dipoles (orientation II dipoles), and thus, orientation I, III, or IV is populated. But, as long as the dipole moment for orientation II is larger than the orientation I, III, or IV dipole moment, the orientation favored at the lowest of temperatures is always orientation II, regardless of the initial seeding of the lattice. This was not quite the case when all dipole moments were taken to be the same,[4] and so the introduction of an orientation-dependent dipole moment improves the agreement between the computer simulation and our observations.

The best fit to the measured orientation distribution is achieved when the dipole moments are assigned as follows: orientation II = 0.7 D and orientation I, III, and IV is ~0.6565 D. This is a 6% difference between the two unique dipole moment magnitudes, i.e., the 0.94 results in Table I.

The 6% difference among the dipole moments results in ~40% of the NH_3D^+ ions assuming orientation II. Since the N–D dipoles are randomly placed on the ammonium sublattice (and do not fill it up very much), the remaining 60% of the population is somewhat randomly distributed among the remaining three orientations (I, III, and IV).

By varying the N–D dipole interactions with orientation, the width of the transition region has been reduced. The IR data show the transition region to be less than 1 order of magnitude at 4% D. In simulations without the orientation-dependent dipole moment, the width of the transition region spans between 3 and 4 orders of magnitude of temperature. But, in simulations with the orientation-dependent dipole moment, the transition region is just a bit more than 1 order of magnitude of temperature wide. Unfortunately, for reasonable values of the N–D dipole moment, the simulated transition is occurring at ~10^{-1} K while the IR-observed transition is centered at ~45 K. As already mentioned, this indicates that our model of the interionic forces is incomplete.

In summary, we have shown that a simple model of orientation-dependent N–D dipoles interacting on a Tutton salt lattice can account for the orientational order–disorder transition we observed. The Monte Carlo simulation provides a way of exploring the details of the N–D dipole interaction driving the order transition. It also provides a way of discovering the structure of the dipole interaction network. The version of the model that yielded the best fit to the IR data showed that there is a 6% difference between the effective dipole moment of an NH_3D^+ ion in orientation II and an ion in orientations I, III, or IV. This 6% dipole asymmetry agrees with the general asymmetry of N–H bond properties for Tutton salt ammonium ions.

Examination of the structure of the calculated system at low temperature suggests that it is an orientational glass; that is, the dipole are frozen in arrangements that depend on the local environment (the arrangement of the nearby NH_3D^+ ions). Note, however, that the "glass" does have partial order.

IV. Kinetics

A. Introduction and Kinetic Equations. The NH_3D^+ ions can reorient in a number of ways. Each of the four orientations of an ion can jump to one of the three others. The reorientation is then characterized by 12 independent first-order rate constants. To determine all of these 12 constants would require much more data than we have obtained from the experiments described below. Therefore, we make the simplifying assumption of C_{3v} symmetry (Figure 2) based on the observed unique role of orientation II. This model gives three independent rate constants.

The kinetics problem for four "chemical components" reacting via 12 first-order steps leads to a set of 4 first-order coupled differential equations. These equations are analogous to those routinely solved for the normal coordinate problem and have been considered by Matsen and Franklin.[10] They are

$$A_i + \sum_{j=1}^{4} K_{ij}A_j = 0 \qquad i = 1, 2, 3, 4 \qquad (1)$$

(9) Binder, K.; Young, A. P. *Rev. Mod. Phys.* **1986**, *58*, 801–976, Section IIC and the references therein.

(10) Matsen, F. A.; Franklin, J. L. *J. Am. Chem. Soc.* **1950**, *72*, 3337–3341. Some of the indexes in this paper are reversed. Also, it is implied that the transformation matrix is real-orthogonal, which is true only in special cases. For a discussion of the use of symmetry, see also: Williams, G.; Cook, M. *Trans. Faraday Soc.* **1971**, *67*, 990–998.

where

$$K_{ij} = -k_{ij} \qquad i \neq j \tag{2}$$

and

$$K_{ii} = \sum_{p=1}^{4} k_{ip} \tag{3}$$

and k_{ji} is the rate constant for site j to site i. The solutions to these differential equations are of the form

$$A_i = \sum_{r=1}^{4} C_{ir} e^{-\lambda_r t} \tag{4}$$

The values of the concentrations measured as a function of time in a kinetics experiment, A_i (in our case, the intensities of the N–D stretching bands or equivalently the occupancy of the four different NH_3D^+ orientations), can be thought of as linear combinations of a set of mutually orthogonal concentrations or "eigenconcentrations",[10] C_r.

Substituting the set of rate constants shown in Figure 2 into eq 1 and solving the system of equations yields the following eigenvalues and corresponding (nonnormalized, nonorthogonal) eigenvectors:

$$\lambda_1 = k_o + 3k_i, \text{ eigenvector: } \begin{bmatrix} k_o/3k_i \\ -1 \\ k_o/3k_i \\ k_o/3k_i \end{bmatrix} \quad A_2 \ (C_{3v} \text{ symmetry}) \tag{5}$$

$$\lambda_{2 \text{ or } 3} = k_o + 3k_a, \text{ eigenvectors: } \begin{bmatrix} 1 \\ 0 \\ 0 \\ -1 \end{bmatrix} \text{ and } \begin{bmatrix} -1/2 \\ 0 \\ 1 \\ -1/2 \end{bmatrix} \quad E \ (C_{3v} \text{ symmetry}) \tag{6}$$

$$\lambda_4 = 0, \text{ eigenvector: } \begin{bmatrix} 1 \\ 1 \\ 1 \\ 1 \end{bmatrix} \quad A_1 \ (C_{3v} \text{ symmetry}) \tag{7}$$

where $k_i = k_{\text{in}\rightarrow\text{out}}$, $k_o = k_{\text{out}\rightarrow\text{in}}$, and $k_a = k_{\text{around}}$ (Figure 2). Equation 7 is the condition of microscopic reversibility.

These eigenvectors and eigenvalues yield the following equations for the time dependence of the absorbance of the four N–D stretching bands:

$$A_{\text{N-D II}}(t) = \Delta A_{\text{N-D II}} e^{-\lambda_1 t} + A^{\text{eq}}_{\text{N-D II}} \tag{8}$$

$$A_n(t) = -(1/3)\Delta A_{\text{N-D II}} e^{-\lambda_1 t} + [\Delta A_n + (1/3)\Delta A_{\text{N-D II}}] e^{-\lambda_2 t} + A_n^{\text{eq}} \tag{9}$$

n = N–D I, N–D III, or N–D IV

$$\Delta A_i = A_i^{\circ} - A_i^{\text{eq}}$$

$$A_i^{\circ} = A_i \ (t = 0) \qquad A_i^{\text{eq}} = A_i \ (t = \infty)$$

Equations 8 and 9 were used to analyze the time response of the N–D stretching absorptions in either the T-jump or hole-burning experiments. Note that the population in orientation II exhibits simple exponential kinetics, but the population in orientation I, III, or IV shows more complex (possibly nonmonotonic) behavior.

We calculated λ_1 by fitting the raw kinetics data from the reequilibration of N–D II to eq 8. Then, we calculated λ_2 by using λ_1 and fitting the raw kinetics data from the reequilibration of N–D I to eq 9. The errors in λ_1 and λ_2 were calculated from the linear fits in the standard manner. Finally, the equilibrium concentrations[4] of II to I, III, and IV were used to give a third condition at each temperature, and k_i, k_o, and k_a were solved for.

The orientational distribution was disturbed in three distinct ways. The first was to hole-burn band I, and this led to values of λ_1 and λ_2 as described above. The second was to burn band II. This leads only to a value of λ_1 since the λ_2 term in eq 9 is zero in the approximation that sites I, III, and IV are equivalent. The T-jump experiment changes mainly orientation II versus the set I, III, IV, and gives the same information as hole-burning band II. We used the T-jump experiment at higher temperatures, where the hole-burning is more difficult.

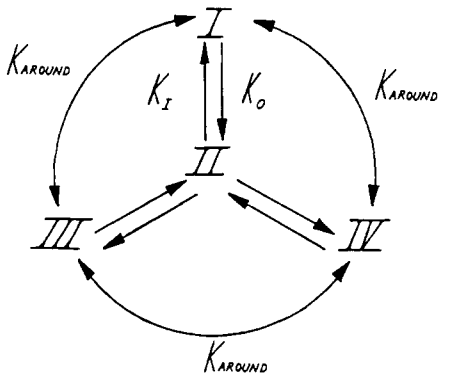

Figure 2. The 12 rate constants that connect the four orientational sites of the NH_3D^+ ion. Orientation II is unique and chosen as the hub of an approximate kinetic scheme in which the other three orientations are taken as equivalent. This yields three independent rate constants. (The three "outer" orientations are not crystallographically equivalent, but their kinetic behavior is similar.)

B. Phonon-Assisted Tunneling. The four NH_3D^+ orientations are inequivalent, and we expect that each of the orientations will have a different energy (the energy we consider is of the NH_3D^+ in the lowest energy level of each orientational well). These energy differences are probably of the order of a few tens of wavenumbers. To go from one orientation to another, the ammonium ion must tunnel and then gain or lose energy by interaction with phonons. The interaction with the phonons can lead to the direct absorption or emission of a phonon or a more complicated "Raman" process.[11] In this process, two unequal phonons are involved with one absorbed and one emitted to make up the energy difference. Detailed models of asymmetric double-well system undergoing tunneling have been considered by Sussman.[13,14] His model consists of two overlapping harmonic oscillators. The phonons can modulate either the distance between the wells or their height. The biggest unknown in these models is the exact form of the lattice modes, and thus the coupling parameter that determines by how much a phonon modulates either the separation or the energy of the wells.

The temperature dependence to be expected from the tunneling process depends on the relative magnitude of the three energy parameters in the problem: the thermal energy (kT), the energy mismatch between the wells (μ_o), and the Debye energy ($k\theta_D$) which characterizes the phonons. There is a fourth energy in the problem, the height of the barrier. This is $\sim$4 kcal/mol (2000 K), sufficiently much greater than the temperatures considered here that we do not have to consider activated processes that go over the barrier.

The Debye temperature is estimated to be greater than 200 K and so we will take $\theta_D \gg T$ in what follows. The various μ_o will turn out to be a few tens of wavenumbers or degrees, as already mentioned, and thus of the same magnitude as T. The temperature dependence of the rate depends on the details of the particular phonon process involved and, since $\mu_o \simeq k_B T$, with the μ_o varying for the particular rate. This leads to a variety of possibilities, and indeed we see different behavior for the different elementary rates.

C. Results. In the hole-burning experiments, we first cooled the ACS sample to the temperature at which we wished to measure its reequilibration kinetics. Next, we created a nonequilibrium NH_3D^+ orientation distribution by structurally hole-burning the N–D I stretch absorption band. An example of the effect of structural hole-burning on the N–D stretching region of the IR spectrum of the salt is shown in Figure 1. After the structural hole-burning had occurred, we monitored the reequilibration of the NH_3D^+ orientations by measuring the IR spectrum of the

(11) Waller, I. *Z. Phys.* **1932**, *79*, 370–388. A textbook discussion of these processes may be found in ref 12.
(12) Abragam, A.; Bleaney, B. *Electron Paramagnetic Resonance of Transition Ions*; Clarendon Press: Oxford, 1970; pp 541–583.
(13) Sussman, J. A. *Phys. Condens. Matter* **1964**, *2*, 146–160.
(14) Sussman, J. A. *Phys. Condens. Matter* **1966**, *4*, 330–335.

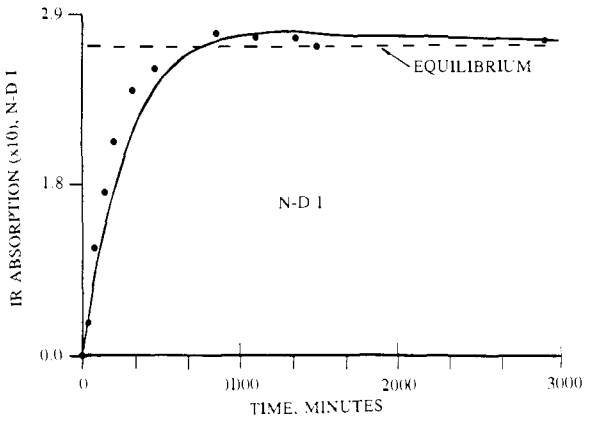

Figure 3. Reequilibration of the N-D I orientation in 4% D ACS at 7.0 K following IR laser irradiation of N-D band I. The laser drives NH_3D^+ ions out of orientation I and into III and IV. The sample was at 7.0 K, but the NH_3D^+ orientation distribution had not yet come to thermal equilibrium. The lack of thermal equilibrium can be compensated for by adjusting the initial conditions used in eq 8 and 9. The graph shows the changes in the integrated intensity (measured above a fitted base line) of N-D band I as a function of time. The black dots are the experimental points, and the dotted line is the equilibrium value of the IR intensity for the band. The solid curve is the theoretical time dependence predicted by eq 9. The laser was turned off at zero time.

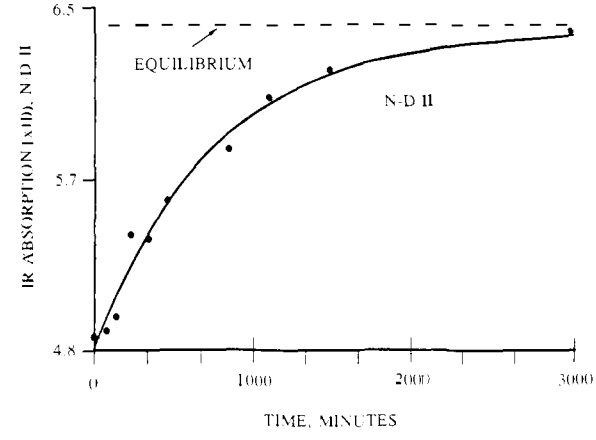

Figure 4. Reequilibration of the N-D II orientation in 4% D ACS at 7.0 K following IR laser irradiation of N-D band I as in Figure 3. The graph shows the changes in the integrated intensity of N-D band II. The black dots are the experimental points, and the dotted line is the equilibrium value of the IR intensity for the band. The solid curve is the theoretical time dependence predicted by eq 8.

sample as a function of time. The experimental equipment and protocol we used for these experiments made it possible to follow the reorientation kinetics over a period of time equal to many time constants.

We observed the hole-burning reequilibration at three temperatures: 7.0, 15.0, and 20.0 K. We fit the data for the time-resolved changes in each of the four N-D bands to eq 8 and 9. Graphs of the experimental and theoretical (assuming C_{3v} rate constant symmetry) reequilibration kinetics for a hole-burning experiment executed at 7.0 K are shown in Figures 3–6. The experimental points for N-D bands I and II fit the theoretical curves well. The sum of exponentials in eq 9 predicts that the reequilibrating N-D I population should overshoot its equilibrium occupancy and approach its equilibrium value from above. The experimental results for N-D I exhibit this type of nonmonotonic behavior. The experimental data for N-D bands III and IV fit the theoretical predictions of eq 9 less well. As the temperature is increased, the quality of the fit of the kinetics of N-D I to eq 9 worsens. This is demonstrated by the increasing error in λ_2. The fit of N-D III to eq 9 is not as good as that of N-D I or N-D IV and shows that C_{3v} symmetry is indeed only an approximation of the true rate constants.

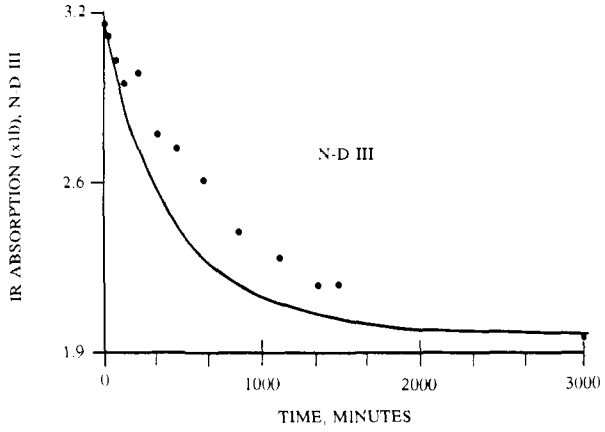

Figure 5. Reequilibration of the N-D III orientation in 4% D ACS at 7.0 K following IR laser irradiation of N-D band I as in Figure 3. The black dots are the experimental points, and the solid curve is the theoretical time dependence predicted by eq 9. The poor agreement between the actual reequilibration rate of the N-D III population and the theoretically predicted rate is probably not due to experimental error but to a breakdown of the assumption of C_{3v} symmetry.

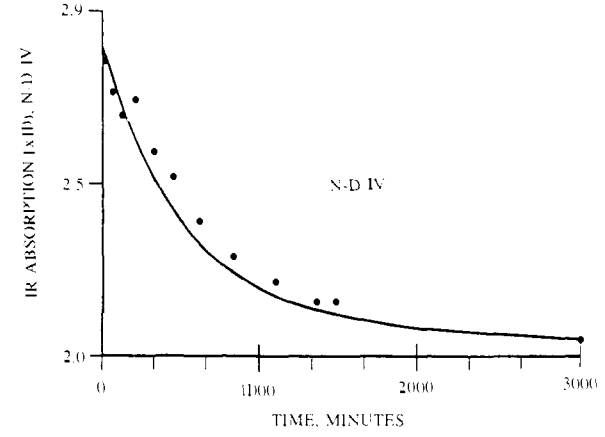

Figure 6. Reequilibration of the N-D IV orientation in 4% D ACS at 7.0 K following IR laser irradiation of N-D band I. The black dots are the experimental points, and the solid curve is the theoretical time dependence predicted by eq 13. The poor agreement between the actual reequilibration rate of the N-D IV population and the theoretically predicted rate is discussed in Figure 5.

Table III. Temperature Dependence of the Exponential Time Constants[a]

temp, K	time constant, h	
	λ_1	λ_2
7.0	12.1 ± 0.5	5.0 ± 0.1
15.0	11.1 ± 0.8	1.9 ± 0.2
20.0	10.0 ± 0.4	1.4 ± 0.2

[a] See eq 8 and 9 for definition of λ_1 and λ_2. The experiments are for ACS doped with 4% D.

Fitting the raw data to eq 8 and 9, respectively, yields two exponential time constants, λ_1 and λ_2, and these are listed in Table III as a function of temperature. As shown in eq 5 and 6, these time constants are sums of the time constants for the elementary NH_3D^+ reorientational motions. With the added knowledge of the value of the equilibrium NH_3D^+ orientation distribution at the given temperatures,[2] λ_1 and λ_2 can be decomposed to give the unique rate constants for the reorientations shown in Figure 2. The values of the rate constants for the three kinds of reorienting motions are listed, as a function of temperature, in Table IV.

D. Discussion. To obtain an order of magnitude estimate of the barrier we start with the simplest possible model—a square barrier. For this, the tunneling rate K is given by[15]

$$K = \nu_s/\pi \exp[-2\pi(l/h)[2\mu(V - E)]^{1/2}] \qquad (10)$$

Table IV. Three Elementary Kinetic Time Constants

temp, K	time constant,[a] h		
	$\tau_{out\rightarrow in}$	$\tau_{in\rightarrow out}$	τ_{around}
7.0	28.3 ± 1.1	63.3 ± 5.0	18.4 ± 1.2
15.0	25.9 ± 1.9	58.0 ± 8.3	6.3 ± 0.5
20.0	23.4 ± 1.0	52.2 ± 4.4	4.3 ± 0.9
35.0	4.0 ± 2.6	4.8 ± 7.7	[b]

[a] The time constant is related to the rate constant by $\tau_x = 1/k_x$. See Figure 2 for the definition of the different rate constants. [b] The 35.0 K time constants are calculated from the T-jump experiments where only the changes in N-D II were measured, and a time constant for the "around" motion could not be calculated.

where ν_s is the attempt frequency, μ the reduced mass, V the height of the square barrier, l the width of the barrier, h Planck's constant, and E the energy of the tunneling system. Since the rotational constant of NH_4^+ in the gas phase is $\sim$5.85 cm^{-1},[16] the rotational constant for rotation of the NH_3D^+ about a pseudo-2-fold axis through the N atom is 4.68 cm^{-1} and for motion about a pseudo-3-fold axis (with the D atom not on the axis) is 4.39 cm^{-1}. In the tunneling we observed, the deuterium atom moves, and in using these rotational constants, we assume that the N atom and the crystal lattice do not. Taking l as 120° and assuming the attempt frequency as that corresponding to a 200-cm^{-1} oscillation, a ($V - E$) of $\sim$4.3 kcal/mol is obtained for a 1/12 h^{-1} tunneling rate (the inverse of the limiting, low-temperature reequilibration time constant). This barrier height is an effective value representing an average of all the different reorientational barriers present on the multiwell, multidimensional potential energy surface of the NH_3D^+ ion in 4% D ACS.

We can obtain estimates of the various orientational barriers by using the 7.0 K time constants for the three unique reorientation reactions (Table IV) and again using eq 10. This calculation yields a model-dependent barrier height of 4.44 ± 0.02 kcal/mol for rotation between orientations I, III, or IV (motion involving k_{around}), a barrier height of 4.54 ± 0.01 kcal/mol for rotation from orientation I, III, or IV to orientation II (motion involving $k_{out\rightarrow in}$), and 4.73 ± 0.02 kcal/mol for rotation from orientation II to orientation I, III, or IV (motion involving $k_{in\rightarrow out}$).

The temperature dependence of the rate constant (or inverse time constant) for a process involving phonon-assisted tunneling is given by[12,13]

$$k = 1/\tau = a \coth (\mu_o/2k_BT) + bT^c \qquad (11)$$

where k is the rate constant, τ is the time constant, a and b are temperature-independent collections of physical constants, μ_o is the energy of the phonon involved in assisting the tunneling ion, T is the ambient temperature, and k_B is Boltzmann's constant. The constants a and b depend on the coupling between the NH_3D^+ and the phonon bath. The temperature dependence of eq 11 derives from the temperature dependence of stimulated emission or absorption among the relevant tunneling levels and the temperature dependence of the phonon density of the crystal. The first term of eq 11 (the coth form) is due to direct processes in which the tunneling ion gains or loses one quantum ($h\nu$) of energy to the phonon bath. The second term arises from phonon scattering or Raman processes.

The value of the exponent c varies with the relative size of the various energy parameters in the system. The value of c is

$$5 \qquad k_B\theta_D \gg \mu_o \gg k_BT \qquad (12)$$

or

$$7 \qquad k_B\theta_D \gg k_BT \gg \mu_o \qquad (13)$$

Since term 2 arises from second-order processes, its contribution is usually small at low temperatures and term 1 dominates the overall rate. There are two important limits of term 1 to examine. The first is when $\mu_o/2k_BT$ is much smaller than one. Then, the coth term may be replaced by k_BT/μ_o. Therefore, when the temperature is high enough so that the thermal energy can readily excite the phonon mode with which the tunneling NH_3D^+ ion is interacting, the rate should exhibit a linear temperature dependence:

$$k = 1/\tau = a'T \qquad \mu_o \ll 2k_BT \qquad (14)$$

where a' includes everything other than temperature. The other important limiting case is when $\mu_o/2k_BT$ is much greater than 1. For this case, the coth term may be replaced with 1. Thus, when the temperature is lowered to the point at which the phonons with which the NH_3D^+ ion interact are not readily thermally excited, the tunneling rate of the NH_3D^+ ion should become temperature independent. Then, a tunneling NH_3D^+ ion can make up the energy mismatch between wells only through the spontaneous emission of phonons.[12]

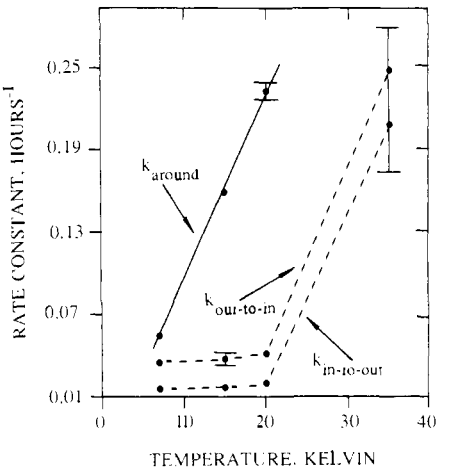

Figure 7. The temperature dependence of the three rate constants shown in Figure 2 and listed in Table IV. The solid line shows the linear temperature dependence of k_{around}. The dotted lines connecting the $k_{out\rightarrow in}$ and $k_{in\rightarrow out}$ data are merely guides to the eye. Below $\sim$20 K, $k_{out\rightarrow in}$ and $k_{in\rightarrow out}$ are relatively temperature independent. Between 30 and 35 K, they rise rapidly. Due to experimental difficulties, we have no data for k_{around} above 20 K. Representative error bars are shown on the graph.

In the temperature range we have examined, the different reorientation rates of the NH_3D^+ ion in ACS exhibit all three types of temperature dependence described above: constant with respect to T, first order in T, and high order in T. This is shown in Figure 7. The rate for k_{around} varies linearly with respect to T (Table IV). This indicates that the phonon mode assisting the tunneling between orientations I, III, and IV is still activated at temperatures below 25 K. Therefore, the phonon must have a frequency of 18 cm^{-1} or less ($\mu_o < 2k_BT$). Since the phonon is assisting the tunneling through a direct process, the asymmetry between the orientation I, III, and IV wells is also less than 18 cm^{-1}. This supports the assumption that orientations I, III, and IV are nearly equivalent in energy.

At low temperatures, the rate constants for reorientational tunneling from orientation I, III, or IV to orientation II ($k_{out\rightarrow in}$), or the reverse reaction ($k_{in\rightarrow out}$), show almost no temperature dependence (Table IV). This temperature independence suggests that phonons that could directly assist this kind of reorientation of the NH_3D^+ ion are not being thermally activated. Thus, the energy mismatch between the orientation II well and the orientation I, III, or IV well is much greater than 18 cm^{-1}. We can obtain another estimate of the mismatch between II and I, III, and IV from the crude estimates of the barrier heights. We had found that the barrier for the II → I, III, IV is 4.73 kcal/mol and that for I, III, IV → II is 4.54 kcal/mol. These numbers would change if a different form of the barrier were assumed. However, using them to indicate the energy differences yields 190 cal/mol (95 K, 66 cm^{-1}). This is considerably larger than 18 cm^{-1} (25 K), as expected. The slight increase in the rates as the temperature

(15) Dennison, D. M.; Hecht, K. T. *Quantum Theory, II. Aggregates of Particles*, Bates, D. R., Ed.; Academic Press: New York, 1962; pp 247–350.
(16) Schafer, E.; Saykally, R. J.; Robiette, A. G. *J. Chem. Phys.* **1984**, *80*, 3969–3977.

increases from 7.0 to 20.0 K is probably due to contributions from indirect processes.

As the temperature is increased above 30 K, the observed reorientation exponential time constants decrease dramatically from ~12 to ~1 h.[4] Such a sharp jump in the temperature dependence of the rate constant usually indicates the onset of Raman phonon-assisted processes.[12] The cross section per phonon for a Raman phonon process is much smaller than that for a direct process, but a direct process involves phonons of only one frequency, while a Raman process involves a sum over phonons of all frequencies. Therefore, when the population of thermally excited phonons rises above a critical level, the second-order Raman processes can become the dominant contribution to the overall rate (eq 11). Once Raman processes are the dominant phonon-assisted mechanism, their high-power temperature dependence can create the kind of sharp temperature increase seen in the NH_3D^+/ACS system.

In eq 12 and 13, we wrote the temperature dependence of the Raman term as T^c, where $c = 5$ is the predicted temperature dependence for $k_B\theta_D \gg \mu_o \gg kT$. The first of these inequalities is well satisfied, the second relies on our estimate of the in–out energy difference of 95 K. It would be of interest to experimentally determine the detailed temperature dependence of the T^c term, but our present data are not sufficient to do this.

V. Summary, Further Discussion, and Conclusions

We have studied the orientation of NH_3D^+ dilute in ammonium cobalt sulfate as a function of temperature from about 70 to 3 K. The NH_3D^+ sits in an asymmetric site in the crystal, and the four positions of the NH_3D^+ are distinguishable by the different N–D infrared stretching bands to which they give rise. The equilibrium orientation starts out random at 70 K and higher temperatures. As the temperature is lowered, ~40% of the ions fall into orientation II. This percentage remains fixed from 30 K to lower temperatures. In this paper, we have modeled the orientation distribution as a function of temperature as due to the mutual interaction of the dipole moments of the NH_3D^+ ions. Assuming that the dipole moment has a small dependence on orientation due to the participation of the surroundings of each ion, we can reproduce qualitatively the orientation distribution as a function of temperature. The calculations provide a picture of the ordered crystal as a partially ordered orientational glass consisting of small regions of ordered dipoles separated by spacers of disordered dipoles. The model does not reproduce the proper absolute temperature and so further modeling will have to be done to determine the NH_3D^+ interactions, especially those due to short-range forces, correctly.

We have been able to perturb the orientational distribution of the ions by two methods: T-jump and spectral hole-burning. The hole-burning process is of great interest in its own right, and in the future, we will investigate the dependence of the hole-burning efficiency on laser power and line width. For now, we simply take advantage of the ability of the hole-burning process to disturb the equilibrium in a number of independent ways. The T-jump and hole-burning experiments, together with the equilibrium distribution of the orientations, provide enough data to determine the three constants for the interchange of the NH_3D^+ orientations. These three rate constants are an approximation to the true situation since we have assumed that orientations I, III, and IV are equivalent, which is not quite true. We also assume that the reorientation of each ion follows first-order kinetics, even though in our model of the equilibrium orientation we assume that the orientations are coupled. Nonetheless, the kinetic equations derived by using these assumptions do give a good fit to the relaxation data (Figures 3–6).

We find that all the temperature dependences characteristic of a tunneling process at low temperatures are observed. The k_{around} rate constant gives a linear dependence on temperature—a dependence constant with small differences among the energies of the I, III, and IV orientations ($\mu_o < 18$ cm^{-1}).

The $k_{in\rightarrow out}$ and $k_{out\rightarrow in}$ rate constants show both a temperature-independent rate ($T \lesssim 20$ K) and a high-order dependence on T rate ($T > 20$). The low-temperature rate is characteristic of rate processes with $\mu_o > k_BT$, and from a crude fit of the rates to a square barrier tunneling formula, we find $\mu_o \sim 66$ cm^{-1} in agreement with the conclusion of the kinetics. At higher temperatures, we expect that high-order dependence on T will go as T^5, but we do not have sufficient data to determine this exponent.

At this point we note that although we have explained both the equilibrium orientational distribution and the reorientation kinetics, we have done so with different models. In particular, in our model of the equilibrium orientations we have ignored any intrinsic differences in the depth of the orientation wells. Also, as already mentioned, we have ignored many-molecule effects in our kinetic analysis. The individual ionic orientations can, of course, have different energies, and we need not be explicit about the cause of these energy differences to solve the kinetics. However, if the energy differences arise from interactions among the ammonium ions, there should be a distribution of energies for each orientation and the kinetics might not obey simple first-order rules. Careful determination of the rates as a function of deuterium concentration could be used to establish whether there are many-ion effects in the kinetics.

The type of temperature dependence observed in ACS—a low power of T dependence at very low temperature, followed by a high power of T dependence at higher temperatures—is found in many other rate processes characterized by relaxation of a two-level system at low temperatures. An example is the reorientation time for O_2^- in KI studied by Kanzig[17] and discussed by Sussman.[13] In these experiments, the O_2^- sits in the halide ion site. The O_2^- can be made to rotate by stressing the crystal. The reorientation time is linear in T to ~4 K and then goes as progressively higher powers of T. A similar result is obtained for the line width of the spectral hole burned in $KI/ReO_4^-/Rb^+$. The spectral hole is burned at the Re-O asymmetric stretch and the laser excitation is thought to cause the Re-O to rotate.[20] Many examples of the temperature dependence of the relaxation of paramagnetic ions may be found in ref 12.

However, we wish to emphasize that the NH_3D^+/ACS system is particularly well-defined. The position of the heavy atoms is crystallographically well-defined, and the mean position of the hydrogen/deuterium atoms is certainly defined by the usual requirements of hydrogen bonding. The analysis is by observation of the well-resolved infrared bands. The crystal is perturbed in only a very minor way (the substitution of a deuterium for a hydrogen atom) and is hopefully unstrained. This system is thus a good example of a tunneling chemical reaction. In future work, we expect to present similar data for kinetics in other NH_3D^+ crystals such as $(NH_4)_2SO_4$ and NH_4NO_3, with the goal of elucidating the relationship between the hydrogen bonding of the ammonium ion and the tunneling kinetics.

Acknowledgment. This work was supported by the National Science Foundation Grant CHE-83-16674. A.P.T. thanks the IBM Corp. and the Regents of the University of California for fellowships.

Registry No. ACS, 39708-96-8; NH_3D^+, 20396-82-1.

(17) Kanzig, W. *J. Phys. Chem. Solids* **1962**, *23*, 479–499 See also: References 18 and 19.

(18) The system RbX/Ag^+: Kapplan, S.; Lutz, F. *Phys. Rev. B* **1972**, *6*, 1537–1551. Barker, A. S., Jr.; Sievers, A. J. *Rev. Mod. Phys.* **1975**, *47*, S1–S180.

(19) Tunneling defects in solids: Narayanamurti, V.; Pohl, R. O. *Rev. Mod. Phys.* **1970**, *42*, 201–236.

(20) Moerner, W. E.; Chraplyvy, A. R.; Sievers, A. J.; Silsbee *Phys. Rev.* **1983**, *B28*, 7244–7259.